Load carrying capability of regional electricity-heat energy systems: definitions, characteristics, and optimal value evaluation

Hong Liu[a], Yuchen Cao[a], Shaoyun Ge[a,*], Zhengyang Xu[a,*], Chenghong Gu[b], Xingtang He[a]
[a] Key Laboratory of Smart Grid of Ministry of Education, Tianjin University, Nankai District, Tianjin 300072, China
[b] Department of Electronic and Electrical Engineering, University of Bath, Bath, BA2 7AY, UK
Corresponding E-mail address: syge@tju.edu.cn (Shaoyun Ge), xuzhengyang@tju.edu.cn (Zhengyang Xu)

ABSTRACT

Evaluating the load carrying capability of regional electricity-heat energy systems is of great significance to its planning and construction. Existing methods evaluate energy supply capability without considering load characteristics between various users. Besides, the impact of integrated demand response is not fully considered. To address these problems, this paper builds a load carrying capability interval model, which uses reliability as a security constraint and considers integrated demand response. An evaluation method for the optimal load carrying capability considering uncertainties of load growth is proposed. First, this paper defines energy supply capability, available capacity, and load carrying capability. Interval models are built to achieve the visualization display of these indices. Their characteristics are studied and the impact factors of interval boundary are analyzed. Secondly, a two-layer optimization model for the evaluation of optimal load carrying capability is constructed, considering the uncertainties of load growth. The upper-layer model aims at optimizing the sum of load carrying capability benefit, integrated demand response cost, and load curtailment penalty. The lower-layer model maximizes energy supply capability. Thereafter, the lower-layer model is linearized based on piecewise linearization and the least square method. The computation efficiency is greatly enhanced. In the case study, a real regional electricity-heat energy system is used to validate the proposed model and method.

KEYWORDS

Integrated energy system; load carrying capability; energy supply capability; uncertainty; integrated demand response

Nomenclature

Variables and parameters	
b_{ij}	Intercept of the reliability constraint boundary of feeder or heat supply area i and j
c_i	Capacity of feeder or heat supply area i (MW)
C_{ben}	Benefit of the load carrying capability (CNY)
$C_{\text{EDR}}/C_{\text{HDR}}$	Cost of the electric or heat demand response (CNY)
$C_{\text{EDR},i}$	Electric demand response cost of feeder i (CNY)

C_{IDR}	Cost of the integrated demand response (CNY)
C_{LOEE}	Cost of the load curtailment (CNY)
H_m	Heat load of the heat supply area m (MW)
k_{ij}	Slope of the reliability constraint boundary of feeder or heat supply area i and j
k_i	Value of the ith dimension of the normal vector
$k_{\mathrm{EDR}}/k_{\mathrm{HDR}}$	Demand response ratio of electric or heat load
$k_{\mathrm{IDR},i}$	Demand response ratio of feeder or heat supply area i
P_i	Electric load of the feeder i (MW)
$p_{\mathrm{de}}/p_{\mathrm{dh}}$	Price of the electric or heat demand response (CNY)
$p_{\mathrm{e}}/p_{\mathrm{h}}$	Prices of electricity and heat (CNY)
$R_{\mathrm{LOEE,e}}/R_{\mathrm{LOEE,h}}$	Electric or heat LOEE (MWh/a)
$R_{\mathrm{LOEE},i}$	The LOEE of feeder or heat supply area i (MWh/a)
t_n	The nth peak load hour
y_i	Load of the ith dimension of operating point (MW)
$y_{i,j,\max}$	Total power supply capability of feeder i and j
w_i	Response willingness of feeder or heat supply area i
α_n	An coefficient varies from 0 to 1
β_n	Coefficient of the nth variable in the regression equation
$\delta_{\mathrm{e},t}/\delta_{\mathrm{h},t}$	Hourly coefficient of electric load or heat load
$\gamma_{\mathrm{be}}/\gamma_{\mathrm{bh}}$	Energy discount for users participated in electric or heat demand response
$\mu_{\mathrm{loss},i}$	Thermal loss of heat supply area i
$\eta_{\mathrm{eff},i}$	Energy conversion efficiency of heat supply area i
Θ	State space
Ω_{RESI}	Reliable energy supply interval
Ω_{ACI}	Available capability interval
Ω_{LCCI}	Load carrying capability interval
$\Omega^{\mathrm{b}}_{\mathrm{LCCI}}$	The upper boundary of load carrying capability interval
∂_{E}	Set of all electric feeders
∂_{H}	Set of all heat supply areas
$\boldsymbol{L}_{\mathrm{curv},i}$	Load curve of the feeder or heat supply area i
$\boldsymbol{Y}$	Operating point
$\boldsymbol{Y}^0$	Operating point of the existing load
$\boldsymbol{\mu}$	Mean vector
$\boldsymbol{\Sigma}$	Symmetric positive definite matrix
Abbreviations	
ACI	Available capacity interval
CNY	Chinese Yuan
DR	Demand response
ES	Energy station

EDR	Electric demand response
ESC	Energy supply capability
HDR	Heat demand response
IDR	Integrated demand response
IES	Integrated energy system
LOEE	Loss of energy expectation
LCC	Load carrying capability
LCCI	Load carrying capability interval
MC	Marginal cost
MR	Marginal revenue
REHES	Regional electricity-heat energy system
RESI	Reliable energy supply interval

1 Introduction

With the consumption of fossil energy and the deterioration of the environment, many countries take carbon emission control as an important development strategy [1]. Integrated energy system (IES) unifies the planning and dispatching of various energy sources, which is conducive to improving energy efficiency and reducing carbon emissions [2]. It has become a hotspot in the field of energy system research. In distribution networks, the power supply capability describes the capability of distribution networks to supply load under security constraints [3]. This index is important to the distribution network and IESs planning [4]. Evaluating the energy supply capability of IESs can find energy supply bottlenecks and verify the feasibility of planning schemes [5].

Currently, some achievements have been made in evaluating the energy supply capability of IESs. Many methods extend the concept of distribution network security region to IES. Security region model is built to describe the energy supply capability of feeders and pipelines [6-8]. The maximum energy supply capability can be represented by the upper boundary of the security region. Ref. [9] proposed an observation-based method to find the boundaries of security regions of natural gas networks. This paper calculated all operating points by a fixed sampling distance. The boundary was obtained by fitting the critical operating point. Ref. [10] i) proposed a piecewise approximation method to determine security region boundary based on hyperplane, ii) studied the application of security region in the optimal control of IESs. Ref. [11] proposed a steady-state security region solution method for electricity-gas IESs, which employed the nonlinear and nonconvex AC power flow model and the nonlinear gas flow model. Ref. [12] studied the two-time-scale feature of the IES. A complete characterization of the steady-state security region was developed for electricity-gas IESs. The above references take integrated energy flows as security constraints. Further considering the impact of equipment failure on energy supply, Ref. [13] constructed a robust scheduling model for regional electricity-gas IESs, which takes N-1 standard as a security constraint. Ref. [14] constructed a security region model for IESs based on N-1 standard. The security of the operating point was defined by the distance between the operating point and security region boundary. However, the energy supply capability only reflects the scale of load that the system can supply at the

peak period from a capacity perspective. Due to the different load characteristics of users, the system has different supply capability for various users and their combinations. Therefore, it is necessary to extend the concept of energy supply capability and propose the concept of load carrying capability to assess the supply capability of IESs.

Integrated demand response (IDR) enables users to reduce the unimportant load in case of failure or peak load with economic compensations, ensuring continuous supply to important load [15]. Concerning IDR, Ref. [16] proposed a two-stage optimal scheduling method for IESs, which considered translational IDR and reducible IDR in day-ahead and intra-day scheduling respectively. Ref. [17] established a multi-objective optimization model for IES long-term planning, considering IDR and equipment aging. The objective was to optimize the total cost, emissions, and energy losses. Ref. [18] proposed a scheduling model for IESs, considering the coordination of economy and environmental protection, and guided users' energy consumption through price-based IDR. Ref. [19] proposed a robust optimization model for equipment capacity planning, considering IDR and thermal comfort. Ref. [20] built a retail energy market competition model based on a multi-leader-follower game. The application of IDR leads to increased retailers' profit and reduced prosumers cost. The existing research mainly considered the impact of IDR on the economy, emissions, energy efficiency, and other factors to determine the operation scheduling and capacity planning of IESs. In these optimization models, the scales of load supplied by IESs are fixed. If more users participate in the IDR, the energy supply reliability will enhance, and the system can supply more load under a fixed security constraint. Although demand response cost increases, the system can supply more load and obtain more benefit. Therefore, it is important to optimize the IDR ratio to maximize the comprehensive benefit of IESs supplying load.

In the future development of existing IESs, various types of load may not increase evenly according to the existing proportion. Therefore, when calculating the benefit of IESs supplying load in the future, it is necessary to consider the uncertainties of load growth. Concerning uncertainty, Ref. [21] proposed an adaptive robust planning method for IESs, considering energy demand uncertainties. In this paper, the fuzzy c-means clustering method was used to cluster the annual hourly load data and generate several typical load scenarios. Ref. [22] proposed a two-stage stochastic programming method for IESs considering energy price uncertainties. The multi-scenario method was used to describe the uncertainties of energy prices. Ref. [23] built a price-based IDR model for multi-energy industrial prosumer. The uncertainties of energy prices on the day-ahead market was considered. Ref. [24] proposed an optimal scheduling method for IESs considering IDR, which considered the uncertainties of hypothesis and cognition in analyzing the impact of IDR on the system. Ref. [25] proposed an operation scheduling and equipment capacity optimization method based on a two-stage stochastic programming model. The uncertainties of energy demand and renewable energy generation were considered in the model. The existing researches have studied the uncertainties of energy demand, energy price, IDR, renewable energy generation, etc. But the uncertainties of load growth is not fully considered. Moreover, the growth of each type of load involves uncertainty. Its description method is also more complex.

To address the above problems, this paper i) proposes a load carrying capability interval model for regional electricity-heat energy systems (REHES), which uses reliability as a security

constraint and considers integrated demand response, ii) proposes an evaluation method for the optimal load carrying capability considering uncertainties of load growth. The novelties and contributions of this paper are as follows:

1) It defines energy supply capability, available capacity, and load carrying capability. Interval models are built to achieve the visualization display of these indices. Their characteristics are studied and the impact factors of interval boundary are analyzed.

2) A two-layer optimization model for load carrying capability evaluation is constructed. It aims at optimizing load carrying capability benefit, integrated demand response costs, and load curtailment penalty. The uncertainties of load growth are considered in evaluating load carrying capability benefit.

3) The calculation of energy supply reliability is linearized based on piecewise linearization and the least square method so that the lower-layer model is much fast to solve.

The rest of this paper is organized as follows. Section 2 defines energy supply capability, available capacity, and load carrying capability. Their characteristics are studied and the impact factors of interval boundary are analyzed. Section 3 constructs a two-layer optimization model to evaluate the optimal load carrying capability. Section 4 analyzes the result of the case study. Section 5 concludes this paper.

2 Model and characteristic analysis of load carrying capability interval

In REHESs, energy can transfer between feeders and heat supply areas. The energy supply capability and load carrying capability of a REHES is not a set of fixed values. Representing them by intevals is more appropriate. The concepts related to load carrying capability are defined below.

2.1 System description

As shown in Fig.1, a REHES includes a power distribution system, a heat supply system, and energy stations (ES). The external energy input is the high voltage power grid. ESs contain energy conversion equipment and energy storages. The heat and cold are supplied to terminal users through the heat/cold supply network with loop. Since both heat and cold are supplied by pipelines with water as the heat-carrying medium, they are regarded as the same type of load.

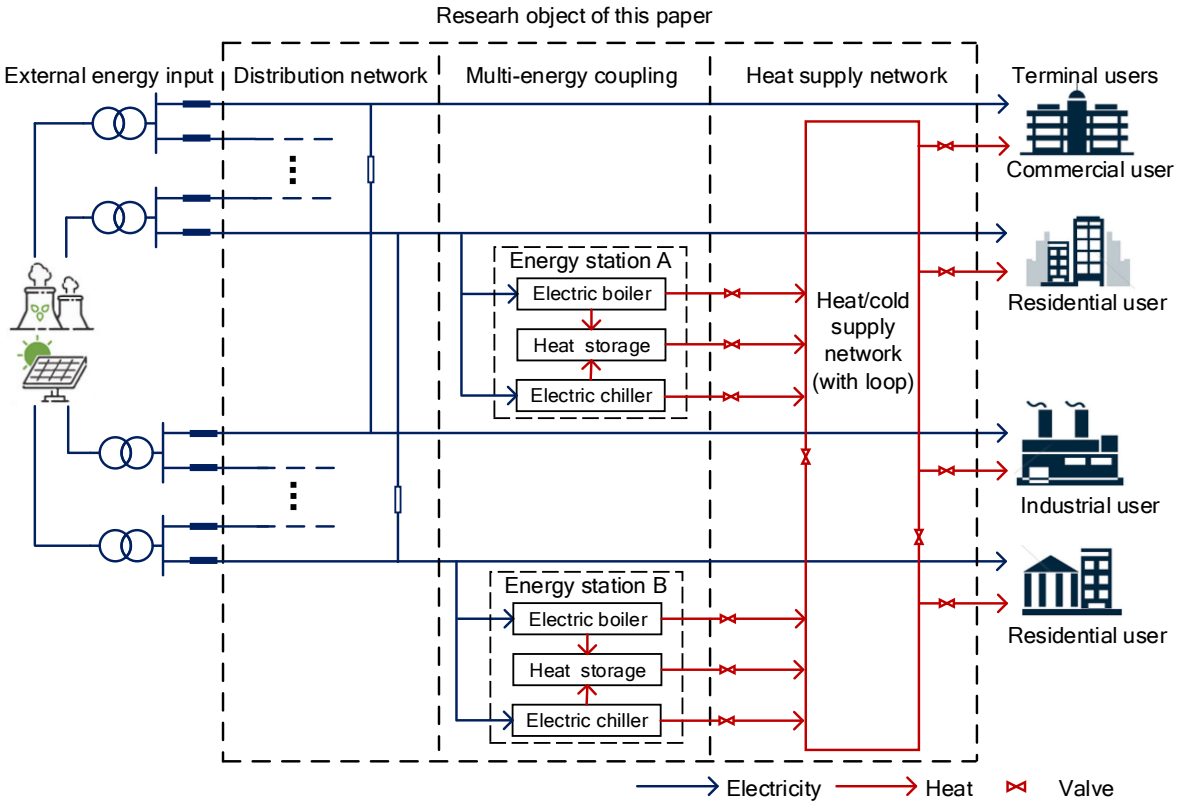

Fig.1 Structure of REHES

2.2 State space

The state space describes all possible operating states of a system. The element of state space Θ is a vector. The vector is a set of the least variables which can completely describe the operating state of the system, and the vector is called the operating point. Because the research object is REHES, the operating point is represented by the loading of each feeder and the outlet pipeline of each heat supply area. The dimension of the operating point equals the number of feeders plus the number of heat supply areas. The operating point can be represented as:

$$\boldsymbol{Y} = (y_1,...,y_n,y_{n+1},...,y_{i+m})^T = (P_1,...,P_n,H_1,...,H_m)^T \tag{1}$$

The state space can be represented as a set of operating points, satisfying capacity constraints:

$$\Theta = \left\{ \boldsymbol{Y} \,|\, f_{\mathrm{st}}(\boldsymbol{Y}) \geq 0 \right\} \tag{2}$$

where $f_{\mathrm{st}}(\boldsymbol{Y})\geq 0$ represents the operating point satisfying the capacity constraints of feeders and pipelines.

The two-dimensional state space is rectangular, representing all possible operating states of the system, as shown in Fig. 2. y_1 and y_2 express the feeders or heat supply areas of REHES. OA and OC express the capacity of y_1 and y_2 respectively.

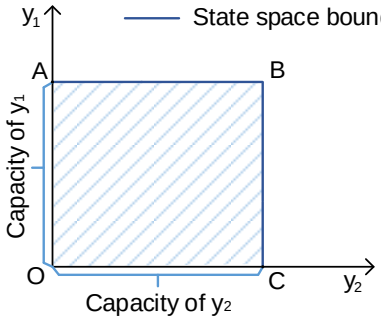

Fig. 2 State space

2.3 Reliable energy supply interval and characteristic analysis

Energy supply capability is defined as the set of load supplied by feeders and outlet pipelines, which satisfies integrated energy flow constraints and reliability constraints. In this paper, the reliable energy supply interval is used to describe the energy supply capability of REHES, represented as:

$$\Omega_{\mathrm{RESI}}=\left\{\boldsymbol{Y}\,\middle|\,\boldsymbol{Y}\in\Theta,\ f_{\mathrm{op}}(\boldsymbol{Y})\geq 0,\ f_{\mathrm{re}}(\boldsymbol{Y})\geq 0\right\} \tag{3}$$

where $f_{\mathrm{op}}(\boldsymbol{Y})\geq 0$ represents the operating point satisfying integrated energy flow constraints. $f_{\mathrm{re}}(\boldsymbol{Y})\geq 0$ represents the operating point satisfying reliability constraints. The specific constraints include power distribution networks, heat supply networks, thermal inertia, operation of energy station, IDR, and reliability. A detailed description of the reliable energy supply interval model can be seen in [26].

The reliable energy supply interval is a subset of the state space, which can be represented by cutting off some operating points according to the state space. The upper boundary of the reliable energy supply interval represents the maximum energy supply capability of the system. If there is no direct connection between the two feeders or heat supply areas, the reliable energy supply interval is rectangular. If there is a direct connection, the shape of reliable energy supply interval may be pentagon, trapezoid, or triangle, as shown in Fig. 3. In Fig. 3(a), OAED is the state space of y_1 and y_2. If the load rates of y_1 and y_2 are both high, the load can not be totally transferred in case of equipment fault. Under the constraint of reliability, the operating points in BCE is not reliable. When the reliability constraint becomes more strict, more operating points will be not reliable. The reliable energy supply interval maybe trapezoid, such as Fig. 3(b), or triangle, such as Fig. 3(c).

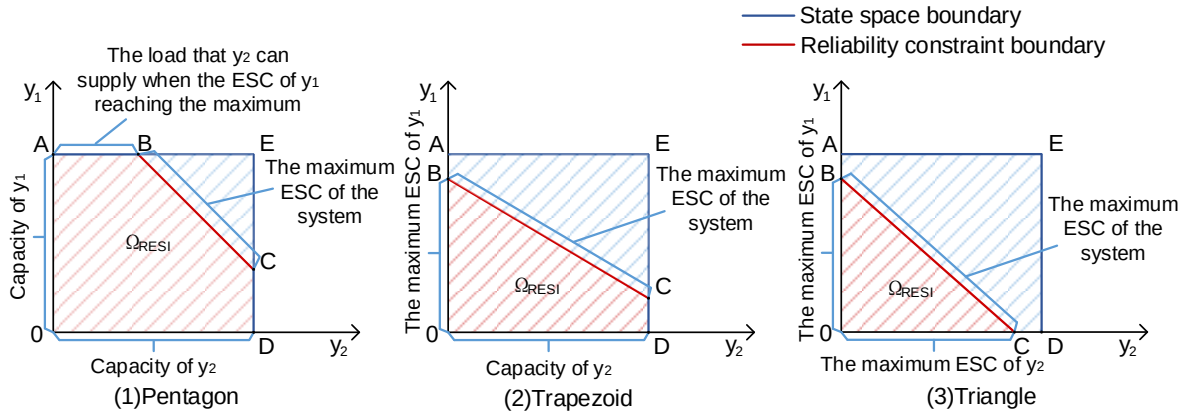

Fig. 3 Reliable energy supply interval

The following part will analyze what factors and how they affect the maximum energy supply capability. For convenience, this paper mainly analyzes the impact factors of two-dimensional and three-dimensional reliable energy supply interval boundaries. The dimension of interval means the number of feeders and the number of heat supply areas in the REHES. The principle of higher dimensional reliable energy supply interval is the same.

(1) Two-dimensional reliable energy supply interval

The upper boundary can be represented by a line segment, as shown in Eq. (4). The variable parameters are slope $-k_{12}$ and intercept b_{12}. For example, in Fig. 3(b), $-k_{12}$ is the slope of the reliability constraint boundary, b_{12} is the length of OB.

$$y_1 = -k_{12} y_2 + b_{12}, y_{2,\min} \le y_2 \le y_{2,\max} \tag{4}$$

When the two dimensions of reliable energy supply interval both express power supply capability, the slope is related to the IDR of the two feeders:

$$k_{12} = \frac{1 - w_2 k_{\mathrm{IDR},2}}{1 - w_1 k_{\mathrm{IDR},1}} \tag{5}$$

where $k_{\mathrm{IDR},i}$ is the IDR ratio of y_i. w_i is the response willingness of y_i.

When the two dimensions both express heat supply capability, the slope is related to the IDR and network losses of the two heat supply areas:

$$k_{12} = \frac{(1 - w_2 k_{\mathrm{IDR},2})(1 - \mu_{\mathrm{loss},1})}{(1 - w_1 k_{\mathrm{IDR},1})(1 - \mu_{\mathrm{loss},2})} \tag{6}$$

where $\mu_{\mathrm{loss},i}$ is the thermal loss of heat supply area i.

When the two dimensions express power and heat supply capability respectively, the slope is related to the IDR, network loss, and energy conversion efficiency:

$$k_{12} = \frac{\eta_{\mathrm{eff},2}(1 - w_2 k_{\mathrm{IDR},2})(1 - \mu_{\mathrm{loss},1})}{1 - w_1 k_{\mathrm{IDR},1}} \tag{7}$$

where $\eta_{\mathrm{eff},i}$ is the energy conversion efficiency of heat supply area i.

The intercept of the line segment is related to reliability constraints and IDR ratios. The relaxation of reliability constraints and the increase of IDR ratios will both lead to the increase of energy supply capability and intercept.

(2) Three-dimensional reliable energy supply interval

When there is no energy transfer or energy coupling between the three dimensions, the reliable energy supply interval is a cuboid:

$$\Omega_{\mathrm{RESI}} = \left\{ (y_1, y_2, y_3) \middle| 0 \le y_1 \le c_1, 0 \le y_2 \le c_2, 0 \le y_3 \le c_3 \right\} \tag{8}$$

where c_1, c_2, and c_3 are the capacities of feeders or heat pipelines.

The maximum energy supply capability can be represented by the outer vertex of the cuboid (c_1,c_2,c_3).

When only two dimensions have an energy transfer or energy coupling relationship, the reliable energy supply interval is a polygonal prism. It may be a triangular prism, trapezoid prism, or pentagonal prism, which can be represented as:

$$\Omega_{\mathrm{RESI}} = \left\{ (y_1, y_2, y_3) \middle| 0 \le y_1 \le c_1, 0 \le y_2 \le c_2, 0 \le y_3 \le c_3, k_1 y_1 + k_2 y_2 \le b_{12} \right\} \tag{9}$$

The maximum energy supply capability can be represented by a line segment:

$$y_1 = -k_{12}y_2 + b_{12}, y_3 = c_3 \tag{10}$$

The expression of the slope of line segment in different scenarios is the same as Eqs (5)-(7).

When all the three dimensions have an energy transfer or energy coupling relationship, the reliable energy supply interval can be represented by the state space cut off by a plane:

$$\Omega_{\mathrm{RESI}} = \left\{(y_1, y_2, y_3) \middle| 0 \le y_1 \le c_1, 0 \le y_2 \le c_2, 0 \le y_3 \le c_3, k_1 y_1 + k_2 y_2 + k_3 y_3 \le b_{123}\right\} \tag{11}$$

The maximum energy supply capability can be represented by the upper boundary, which is a plane, and its normal vector can be represented as:

$$\vec{s} = \left(\frac{1}{k_1}, \frac{1}{k_2}, \frac{1}{k_3}\right) \tag{12}$$

The normal vector is related to the type of energy, IDR, energy conversion efficiency, and network loss of y_1, y_2, and y_3. When y_i expresses power supply capability, the ith dimension of the normal vector can be represented as:

$$\frac{1}{k_i} = 1 - w_i k_{\mathrm{IDR},i} \tag{13}$$

When y_i expresses heat supply capability, the ith dimension of the normal vector can be represented as:

$$\frac{1}{k_i} = \frac{1 - w_i k_{\mathrm{IDR},i}}{\mu_{\mathrm{loss},i}(1 - \eta_{\mathrm{eff},i})} \tag{14}$$

2.4 Available capacity interval

The available capacity is defined as the load of each feeder and heat supply area that can be added for the built REHESs, under the constraints of integrated energy flow and reliability.

For a REHES, the existing load is represented as:

$$\boldsymbol{Y}^0 = (y_1^0, ..., y_n^0, y_{n+1}^0, ..., y_{n+m}^0)^T \tag{15}$$

In this paper, the available capacity interval is used to describe the available capacity of REHESs, which can be represented as:

$$\Omega_{\mathrm{ACI}} = \left\{\boldsymbol{Y} \middle| \boldsymbol{Y} \in \Omega_{\mathrm{RESI}}, y_i \ge y_i^0, \forall 1 \le i \le n+m\right\} \tag{16}$$

According to the definition of available capacity, based on a reliable energy supply interval, take the operating point as the starting point to make straight lines parallel to the coordinate axes. The available capacity interval is the area surrounded by the straight lines, state space boundary, and reliable constraint boundary. As shown in Fig. 4, based on the pentagonal reliable energy supply interval OADEC, the available capacity interval is represented by the shaded area Y^0MDN. Y^0 represents the existing load, Y^0M and Y^0N represents the load that can be added on y_1 and y_2.

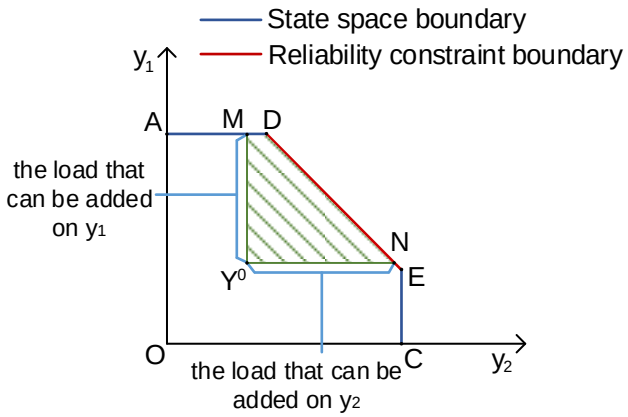

Fig. 4 Available capacity interval

2.5 Load carrying capability interval and characteristic analysis

Further considering load characteristics between various users , the concept of load carrying capability is proposed based on energy supply capability. The load carrying capability is defined as the newly added load of various users that the REHES can supply under the constraints of integrated energy flow and reliability. Because the load characteristics of various users are different, the overall scale of load in an area is not a simple numerical sum of various users.

Load carrying capability interval is used to describe the load carrying capability of REHES, which can be represented as:

$$\Omega_{\mathrm{LCCI}}=\left\{(y_1,y_2,...,y_n)\middle|\boldsymbol{Y}=f_{\mathrm{s}}(y_1,y_2,...,y_n),\boldsymbol{Y}\in\Omega_{\mathrm{RESI}}\right\} \tag{17}$$

where $f_{\mathrm{s}}(y_1,y_2,...,y_n)$ expresses the sum of load considering the differences of load characteristics between various users.

According to the definition of load carrying capability, a two-dimensional load carrying capability interval which both dimensions represent power supply capability can be represented as:

$$\Omega_{\mathrm{LCCI}}=\left\{(y_1,y_2)\middle|0\le y_1\le y_{1,\max},0\le y_2\le y_{2,\max},f_{\mathrm{s}}(y_1,y_2)\le y_{1,2,\max}\right\} \tag{18}$$

The upper boundary of the load carrying capability interval is:

$$f_{\mathrm{s}}(y_1,y_2)=y_{1,2,\max} \tag{19}$$

$f_{\mathrm{s}}(y_1, y_2)$ can be represented as:

$$f_{\mathrm{s}}(y_1,y_2)=\max(y_1\cdot\boldsymbol{L}_{curv,1}+y_2\cdot\boldsymbol{L}_{curv,2}) \tag{20}$$

where $\boldsymbol{L}_{\mathrm{curv},1}$ and $\boldsymbol{L}_{\mathrm{curv},2}$ are load curves of y_1 and y_2 respectively, which are arrays with elements between 0 and 1.

When the load of y_1 and y_2 are added in different proportions, the peak load may occur at different hours. Now construct a new array:

$$\boldsymbol{L}_{curv,1,2}=(1-\alpha)\boldsymbol{L}_{curv,1}+\alpha\boldsymbol{L}_{curv,2},\alpha\in[0,1] \tag{21}$$

When α varies from 0 to 1, $\boldsymbol{L}_{\mathrm{curv},1,2}$ may have 1 to n peak load hours, represents as $(t_1,t_2,...,t_n)$. And we can know the α when the peak load hour changes, represents as $(\alpha_1, \alpha_2,..., \alpha_{n-1})$. When there is only one peak load hour, the boundary $f_{\mathrm{s}}(y_1, y_2)=y_{1,2,\max}$ can be equivalent to:

$$y_1 \cdot \boldsymbol{L}_{curv,1}(t_1) + y_2 \cdot \boldsymbol{L}_{curv,2}(t_1) = y_{1,2,\max} \tag{22}$$

The slope of boundary can be represented as:

$$k = \frac{\partial y_1}{\partial y_2} = -\frac{\boldsymbol{L}_{curv,2}(t_1)}{\boldsymbol{L}_{curv,1}(t_1)} = -1 \tag{23}$$

In this case, the boundary of the load carrying capability interval is a straight line.

When there are several peak load hours, the slope of each section of the boundary is different. When $y_1/y_2 \geq (1\text{-}\alpha)/\alpha_1$, the slope of the corresponding section of the boundary is:

$$k = \frac{\partial y_1}{\partial y_2} = -\frac{\boldsymbol{L}_{curv,2}(t_1)}{\boldsymbol{L}_{curv,1}(t_1)} \tag{24}$$

When $(1\text{-}\alpha_{m+1})/\alpha_{m+1} \leq y_1/y_2 \leq (1\text{-}\alpha_m)/\alpha_m$, $1 \leq m \leq n\text{-}2$, the slope of the corresponding section of the boundary is:

$$k = \frac{\partial y_1}{\partial y_2} = -\frac{\boldsymbol{L}_{curv,2}(t_{m+1})}{\boldsymbol{L}_{curv,1}(t_{m+1})} \tag{25}$$

When $y_1/y_2 \leq (1\text{-}\alpha_{n-1})/\alpha_{n-1}$, the slope of the corresponding section of the boundary is:

$$k = \frac{\partial y_1}{\partial y_2} = -\frac{\boldsymbol{L}_{curv,2}(t_n)}{\boldsymbol{L}_{curv,1}(t_n)} \tag{26}$$

Therefore, the upper boundary of the two-dimensional load carrying capability interval is a broken line. The quantity of segments is equal to the quantity of peak load hours after the load of y_1 and y_2 added in different proportions. The left and right derivatives of the upper boundary function at kink points are different. It means that the load reaches the maximum at two hours at kink points. When the two dimensions of the load carrying capability interval represent different energy sources, the principle is the same, but the energy conversion efficiency needs to be considered when calculating the sum of load.

The visualization display of load carrying capability interval is shown in Fig. 5. Fig. 5(a) shows the load carrying capability interval of y_1 and y_2. Fig. 5(b) shows the load curves of y_1 and y_2. Fig. 5(c)-(f) show the sum of load at point B, point C, point E, and point F respectively. OA and OD express the capacity of y_1 and y_2 respectively. PN and PM express the existing load of y_1 and y_2 respectively. PB and PC express the scale of load can increase when the new added load is only y_1 or y_2 respectively. Point E and point F are two kink points on the boundary. EE″ and EE′ express the new added load of y_1 and y_2 at the point E respectively. FF″ and FF′ express the new added load of y_1 and y_2 at the point F respectively.

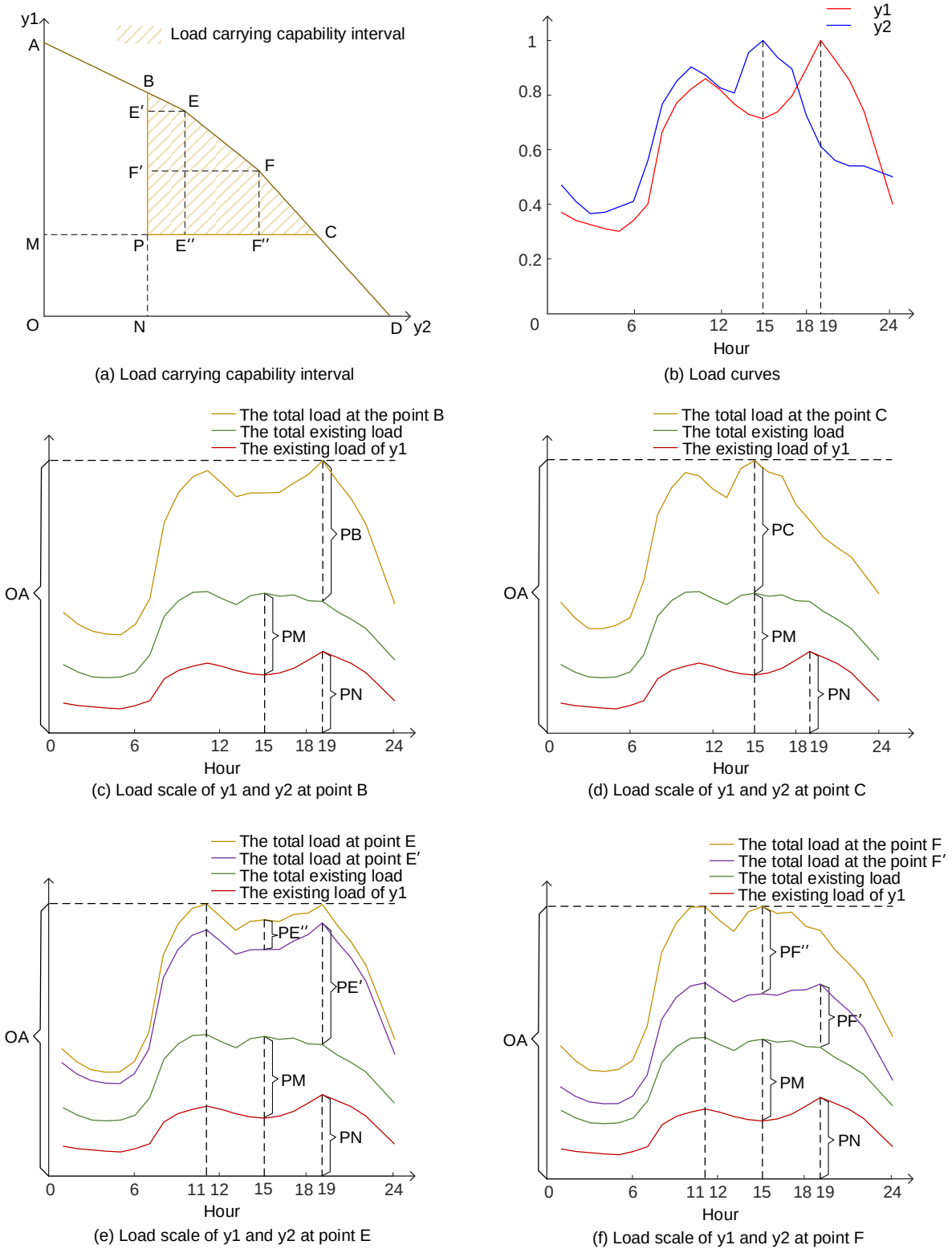

Fig. 5 Load carrying capability interval

3 Evaluation of optimal load carrying capability for REHESs

According to the analysis of the impact factors of interval boundary in Section 2, relaxing reliability constraints and increasing IDR ratios will increase the energy supply capability of

the system, to improve the benefit of load carrying capability. However, relaxing reliability constraints will lead to the increase of load curtailment penalty, and increasing IDR ratios will lead to the increase of demand response cost. Therefore, the evaluation of optimal load carrying capability is of important meaning to the planning of REHESs.

3.1 Model of optimal load carrying capability evaluation considering uncertainties of load growth

(1) Model framework

The purpose of this section is to solve the reliability constraints and IDR ratios when the operation economy reaches the optimum. The objective of the upper-layer model is the optimal operation economy. The optimization variables are reliability constraints and IDR ratios. The lower-layer model calculates the maximum energy supply capability according to the reliability constraints and IDR ratios output by the upper-layer model. When calculating the operation economy, the benefit of energy sales is related to the load scale of various users, not how much load the system can supply. Therefore, when the lower-layer model returns data, the upper-layer model needs to convert the energy supply capability into load carrying capability. The model framework is shown in Fig. 6.

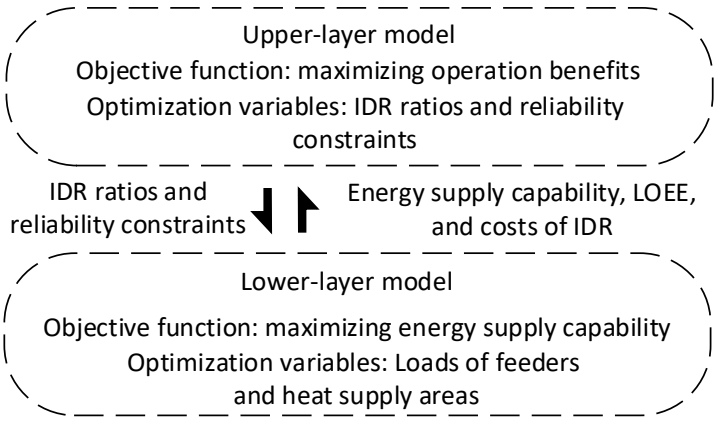

Fig. 6 Two-layer model framework

(2) Load carrying capability benefit calculation considering uncertainties of load growth

The benefit of load carrying capability is calculated according to the maximum load of various users that can be supplied. In the future development of the existing IESs, various types of load may not increase evenly according to the existing proportion. Therefore, the uncertainties of load growth needs to be considered in the benefit calculation. According to the definition of load carrying capability in Section 2.5, each point on the boundary of load carrying capability interval corresponds to a possible future scenario. The benefit of load carrying capability considering uncertainties can be obtained by calculating the benefit and probability of each point on the boundary of load carrying capability interval.

It is assumed that the scale of existing load is $\boldsymbol{Y}^0=\left(Y_1^0,Y_2^0,...,Y_n^0\right)'$, and a point on the boundary of load carrying capability interval is $\boldsymbol{Y}=\left(Y_1,Y_2,...,Y_n\right)'$. The multivariate normal distribution probability density function of $\boldsymbol{Y}$ can be established to describe the uncertainties of load growth. According to the definition of multivariate normal distribution, if a random vector

$\boldsymbol{X}_{p\times1}=\left(X_1,X_2,...,X_p\right)'$ is a p-dimensional normal random vector, the $\boldsymbol{X}$ has a probability density function [27,28]:

$$f\left(\boldsymbol{X}\right)=\frac{1}{\left(2\pi\right)^{\frac{p}{2}}\left|\boldsymbol{\Sigma}\right|^{\frac{1}{2}}}\exp\left\{-\frac{1}{2}\left(\boldsymbol{X}-\boldsymbol{\mu}\right)'\boldsymbol{\Sigma}^{-1}\left(\boldsymbol{X}-\boldsymbol{\mu}\right)\right\},\boldsymbol{X}\in R^p \tag{27}$$

where $\boldsymbol{\mu}$ is the expectation vector, $\boldsymbol{\mu}=\left(\mu_1,\mu_2,...,\mu_p\right)'$. $\boldsymbol{\Sigma}=\operatorname{cov}\boldsymbol{X}$ is the symmetric positive definite matrix, represents the covariance between random vectors.

For the vector $\boldsymbol{Y}=\left(Y_1,Y_2,...,Y_n\right)'$, the nth variable can be obtained if n-1 variables are known. $\boldsymbol{Y}$ obeys n-1 normal distribution, $\boldsymbol{Y}\sim N_{n-1}\left(\boldsymbol{\mu},\boldsymbol{\Sigma}\right)$. Since there is no correlation between n-1 variables and the variance of each variable is the same, its symmetric positive definite matrix can be represented as:

$$\boldsymbol{\Sigma}=\begin{pmatrix}\sigma & 0 & & 0\\ 0 & \sigma & & 0\\ & & \ddots & \\ 0 & 0 & & \sigma\end{pmatrix}_{(n-1)\times(n-1)} \tag{28}$$

In this question, $\left(\boldsymbol{Y}-\boldsymbol{\mu}\right)'\left(\boldsymbol{Y}-\boldsymbol{\mu}\right)$ expresses the distance from the point $\boldsymbol{Y}$ on the boundary to the vector representing the existing load:

$$\left(\boldsymbol{Y}-\boldsymbol{\mu}\right)'\left(\boldsymbol{Y}-\boldsymbol{\mu}\right)=\frac{\left|\boldsymbol{Y}\times\boldsymbol{Y}^0\right|}{\left|\boldsymbol{Y}^0\right|} \tag{29}$$

In summary, the probability density function of $\boldsymbol{Y}$ on R^n can be established:

$$f_{\mathrm{p}}\left(\boldsymbol{Y}\right)=\frac{1}{\left(2\pi\right)^{\frac{n-1}{2}}\sigma^{\frac{n-1}{2}}}\exp\left\{-\frac{1}{2\sigma^{n-1}}\cdot\frac{\left|\boldsymbol{Y}\times\boldsymbol{Y}^0\right|}{\left|\boldsymbol{Y}^0\right|}\right\},\boldsymbol{Y}\in R^n \tag{30}$$

Because the load carrying capability interval is n-dimensional bounded, the integral of the existing probability density function on the boundary is less than 1. It is necessary to modify the probability density function of $\boldsymbol{Y}$ on the boundary $\Omega_{\mathrm{LCCI}}^{\mathrm{b}}$ as follows:

$$f_{\mathrm{p}}'\left(\boldsymbol{Y}\right)=\frac{f_{\mathrm{p}}\left(\boldsymbol{Y}\right)}{\iint_{\Omega_{\mathrm{LCCI}}^{\mathrm{b}}}f_{\mathrm{p}}\left(\boldsymbol{Y}\right)} \tag{31}$$

The load carrying capability benefit is calculated:

$$C_{\mathrm{ben}}=\iint_{\Omega_{\mathrm{LCCI}}^{\mathrm{b}}}f_{\mathrm{p}}'\left(\boldsymbol{Y}\right)\cdot R\left(\boldsymbol{Y}\right) \tag{32}$$

where $R(\boldsymbol{Y})$ is a function of calculating the energy sales benefit according to energy prices of different types of users.

(3) Upper-layer model

The objective function is the comprehensive optimization of load carrying capability benefit, IDR costs, and load curtailment penalty:

$$F = \max(C_{\text{ben}} - C_{\text{IDR}} - C_{\text{LOEE}}) \tag{33}$$

The load carrying capability benefit is calculated in Eq. (32). IDR costs contain the cost of electric demand response (DR) and heat DR:

$$C_{\text{EDR}} = p_{\text{de}} \sum_{t=1}^{8760} \delta_{\text{e},t} P_{\text{re},i} + \gamma_{\text{be}} p_{\text{e}} \sum_{t=1}^{8760} \delta_{\text{e},t} P_i - p_{\text{pe}} \sum_{t=1}^{8760} \delta_{\text{e},t} (P_{\text{dr},i} - P_{\text{re},i}) \tag{34}$$

$$C_{\text{HDR}} = p_{\text{dh}} \sum_{t=1}^{8760} \delta_{\text{h},t} H_{\text{re},m} + \gamma_{\text{bh}} p_{\text{h}} \sum_{t=1}^{8760} \delta_{\text{h},t} H_m - p_{\text{ph}} \sum_{t=1}^{8760} \delta_{\text{h},t} (H_{\text{dr},m} - H_{\text{re},m}) \tag{35}$$

The load curtailment penalty is related to reliability constraints and the penalty price of load curtailment:

$$C_{\text{LOEE}} = \sum_{i}^{n} p_{\text{panel},i} R_{\text{LOEE},i} \tag{36}$$

The constraints of the upper-layer model are the value range of reliability constraints and IDR ratios

$$0 \le k_{\text{EDR}} \le k_{\text{EDR,max}} \tag{37}$$

$$0 \le k_{\text{HDR}} \le k_{\text{HDR,max}} \tag{38}$$

$$R_{\text{LOEE,e,max}} \ge 0 \tag{39}$$

$$R_{\text{LOEE,h,max}} \ge 0 \tag{40}$$

(4) Lower-layer model

The lower-layer model calculates maximum energy supply capability. Considering the ratio of electric load to heat load in each area is fixed in the actual situation, the objective function is:

$$F = \max(\sum_{i \in \partial E} P_i + \sum_{j \in \partial H} H_j) \tag{41}$$

The constraints include power distribution networks, heat supply networks, thermal inertia, operation of ES, IDR, and reliability. The detailed constraints can be seen in [26].

The calculation of reliability involves energy transfer, load reduction, and other factors. The IDR costs also need to be calculated. It is a very complex nonlinear problem, and the lower-layer model cannot be solved by linear programming solvers. Besides, calculating reliability based on the Monte Carlo simulation is long time-comsuming. To improve the computation efficiency of the model, the lower-layer model needs to be linearized. In this paper, the upper-layer model is solved using a genetic algorithm, and the lower-layer model is solved by the CPLEX solver.

3.2 Linearization method

(1) Reliability calculation

Taking the loss of energy expected (LOEE) of a feeder as an example, it can be linearized

based on a piecewise linearization method. When the feeder i and its connected feeder j meet the N-1 constraint, only the load of the fault area will be curtailed in case of failure. The LOEE of feeder i is only related to the load P_i. The linear regression can be established:

$$R_{\mathrm{LOEE},i} = \beta_1 \cdot P_i \tag{42}$$

When the N-1 constraint is not satisfied, assuming that a fault occurs during the peak load period, some load will not be transferred, resulting in load curtailment. The LOEE of feeder i is related to the load of feeders i and j, and the electric DR ratio. If the load of feeders i and j increase, the load cannot be transferred and the time that the N-1 constraint is not satisfied will both increase. The LOEE of feeder i can be represented by a polynomial regression:

$$R_{\mathrm{LOEE},i} = \beta_0 + \beta_1 \cdot P_i + \beta_2 \cdot P_j + \beta_3 \cdot k'_{\mathrm{EDR}} P_i^2 + \beta_4 \cdot k'_{\mathrm{EDR}} P_i P_j + \beta_5 \cdot k'_{\mathrm{EDR}} P_j^2 \tag{43}$$

$$k'_{\mathrm{EDR}} = 1 - k_{\mathrm{EDR}} \tag{44}$$

Similarly, when heat supply area i and its connected heat supply areas meet the N-1 constraint, the LOEE of heat supply area i is only related to its heat load H_i:

$$R_{\mathrm{LOEE},i} = \beta_1 \cdot H_i \tag{45}$$

When the N-1 constraint is not satisfied, the LOEE of heat supply area i is related to its heat load H_i, the heat load of its connected heat supply areas H_j, electrical load of the feeder connected to the ES P_j, and heat DR ratio:

$$R_{\mathrm{LOEE},i} = \beta_0 + \beta_1 \cdot H_i + \beta_2 \cdot H_j + \beta_3 \cdot H_i P_j + \beta_4 \cdot H_j P_j + \beta_5 \cdot k'_{\mathrm{HDR}} H_i^2 + \beta_6 \cdot k'_{\mathrm{HDR}} H_i H_j + \beta_7 \cdot k'_{\mathrm{HDR}} H_j^2 \tag{46}$$

$$k'_{\mathrm{HDR}} = 1 - k_{\mathrm{HDR}} \tag{47}$$

After determining the regression equation of LOEE, the reliability is calculated by the Monte Carlo simulation method [29]. The coefficients of the regression equation are calculated by the least square method [30].

(2) IDR costs calculation

The principle is similar to the linearization method for reliability calculation. When the IDR ratios are 0, the IDR costs are 0, and thus there are no constant terms in the regression equation. Taking a feeder as an example, its electric DR cost can be linearized as:

$$C_{\mathrm{EDR},i} = \beta_1 \cdot k_{\mathrm{EDR}} P_i + \beta_2 \cdot k_{\mathrm{EDR}} P_j + \beta_3 \cdot k_{\mathrm{EDR}} P_i^2 + \beta_4 \cdot k_{\mathrm{EDR}} P_i P_j + \beta_5 \cdot k_{\mathrm{EDR}} P_j^2 \tag{48}$$

4 Case study

4.1 Case overview

In this paper, the improved IEEE RBTS bus 2 test sytem [31] and Barry Island heating network [32] are used in this study to construct a REHES test system. The network structure is shown in Fig. 7. The equipment of each ES contains an electric boiler, an electric chiller, and a heat storage. The parameters of equipment are shown in Table 1. The load curves of various users are shown in Fig. 8. Based on the practical condition, ESs supply heat load from November 1 to April 1 of the next year, supply cooling load in the rest of time. The IDR

willingness of resident users is 0.8, commercial users is 0.5, and industrial users is 0.35. The energy price of resident users is 0.5CNY/kWh, the energy price of commercial and industrial users is 0.7CNY/kWh, the discount for participating in IDR is 3%, and the penalty of breaching IDR contracts is 1.0CNY/kWh. The penalty of electricity shortage is 20 times of electricity price. The penalty of heat shortage is 10 times of heat price

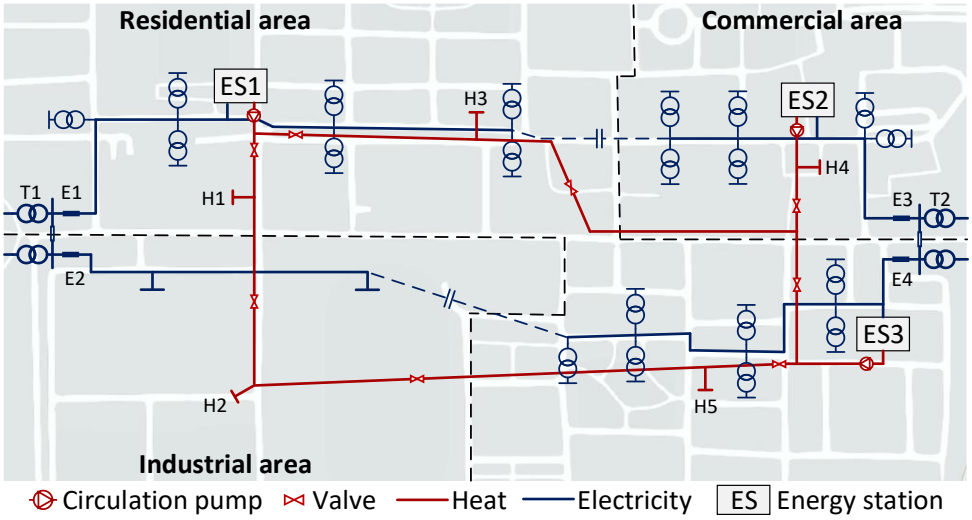

Fig. 7 Network structure of the REHES

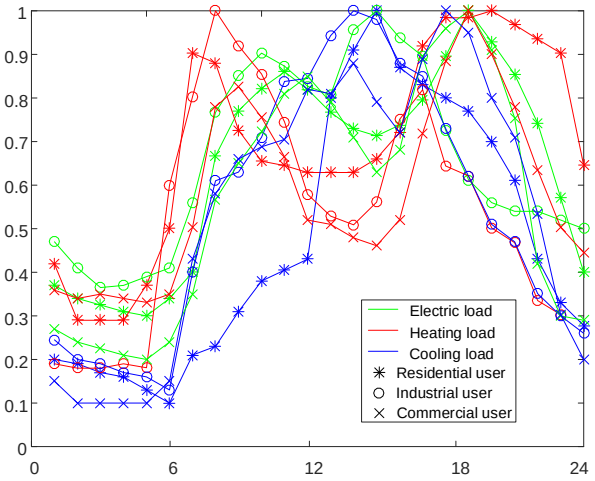

Fig. 8 Load curves of various users

Table 1. Parameters of the REHES equipment

Equipment	Capacity	Failure rate(f/a)	Mean repair time(h)
Electric feeder	8.66MVA	0.065/km	10
Thermal pipeline	160kg/s	0.08/km	10
Main transformer	10MVA	0.015	30
Breaker	25kA	0.006	10
Electric boiler	6MW	1	20
Electric chiller	6MW	1	20
Heat storage	2MWh	-	-

4.2 Result of reliable energy supply interval and load carrying capability interval

(1) Reliable energy supply interval

When the LOEE of electricity and heat are constrainted less than 30MWh/a and 120MWh/a respectively, and the IDR ratios of electric load and heat load are 10% and 15% respectively, the points on the boundary are calculated and fitted to obtain the reliable energy supply interval, shown in Fig. 9. In the figure, the rectangle OABC represents the state space. The pentagon OADEC represents the reliable energy supply interval (RESI). The line segments OA and OC represent that the capacities of feeders 1 and 3 are 8.66MW. AD represents that feeder 3 can supply 2.35MW electric load while the energy supply capability (ESC) of feeder 1 reaches the maximum. DE is the upper boundary of the reliable energy supply interval, represents the maximum energy supply capability of feeders 1 and 3.

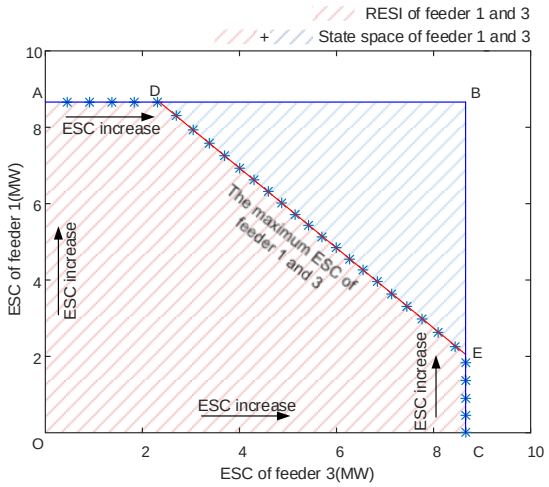

Fig. 9 Reliable energy supply interval

(2) Available capacity interval and load carrying capability interval

It is assumed that the existing load of feeders 1 and 3 are both 3MW. The available capacity interval (ACI) and load carrying capability interval (LCCI) are shown in Fig. 10. In the figure, $\boldsymbol{Y}^0$ represents the existing load. It can be seen that after considering the load characteristics, the load carrying capability is greater than the available capacity, since the load characteristics of feeders 1 and 3 are complementary.

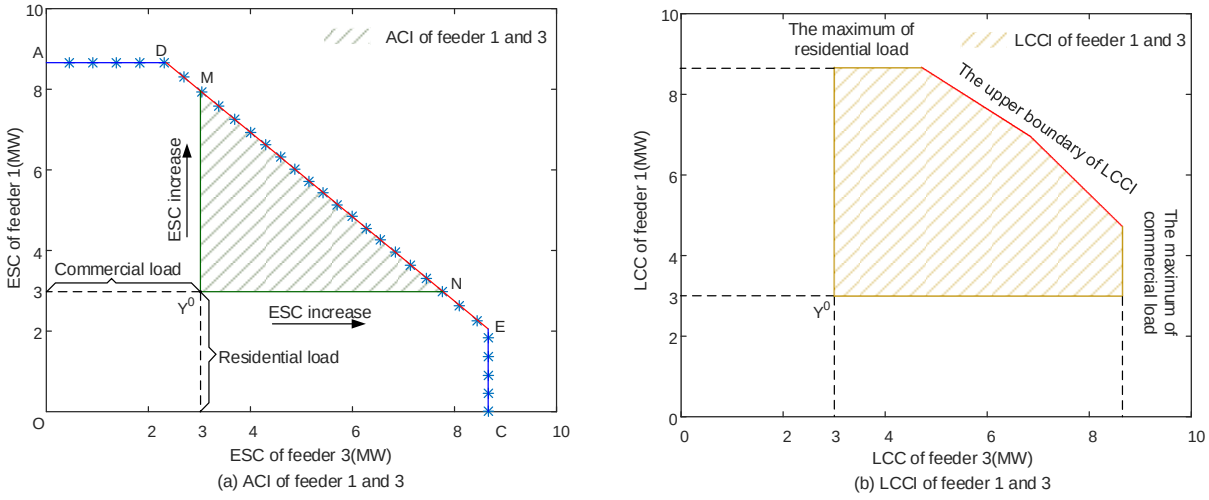

Fig. 10 Available capacity interval and load carrying capability interval

(3) Slope of reliable energy supply interval upper boundary

According to the analysis in Section 2.3, the theoretical slope of the boundary is -1.033. In

the case study, the fitted boundary slope is -1.047. The error is 1.36%. It can be interpreted that the error is caused by randomly generating sampling points and calculating regression function in the linearization process of reliability calculation. The error is small, which can still prove the effectiveness of the method.

4.3 Result of optimal load carrying capability

In the case study, feeders 1 and 4 supply residential users, the ratio of electric load to heat load is 0.6. Feeder 2 supplies commercial users, the ratio of electric load to heat load is 0.5. Feeder 3 supplies industrial users, the ratio of electric load to heat load is 0.2. The existing load of feeders 1-4 and heat supply areas 1-5 is [3,3,3,3,0.9,0.6,0.9,1.5,1.8]MW.

According to the method proposed in Section 3.1, it is obtained that when the operating benefit reaches the maximum, the reliability constraints of electricity and heat are 53.9MWh/a and 45.3MWh/a respectively, the DR ratios of electricity and heat are 10.2% and 9.8% respectively. The maximum operating benefit is 48.71 Million CNY, the load carrying capability benefit is 50.00 Million CNY, the IDR cost is 0.37 Million CNY, and the load curtailment penalty is 0.92 Million CNY.

(1) Relationship between reliability constraints and load carrying capability benefit

Through the relationship between marginal cost (MC) and marginal revenue (MR), the impact of reliability constraints on load carrying capability benefit is analyzed. Fixed the DR ratios of electricity and heat to 10.2% and 9.8% respectively, the relationship between reliability constraint of electricity and load carrying capability benefit is calculated when the reliability constraint of heat is set to 45.3MWh/a, 30MWh/a, and 60MWh/a respectively. It is shown in Fig. 11.

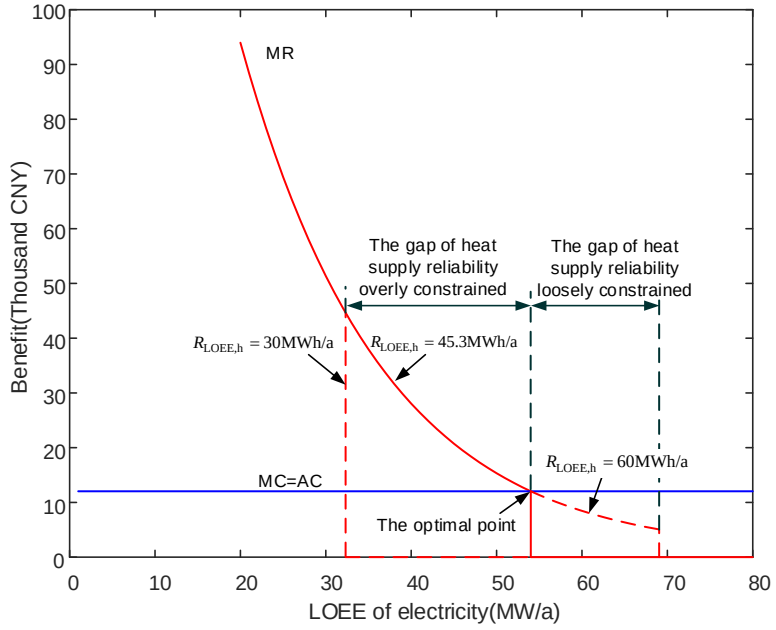

Fig. 11 The relationship between reliability constraint and load carrying capability benefit

Because the penalty of load curtailment is fixed, when the reliability constraint of electricity changes, the MC of the system is fixed and equals the average cost. When the reliability constraint of heat is 45.3MWh/a, the MR decreases with the relaxation of the reliability

constraint of electricity. Until the reliability constraint of electricity is 53.9MWh/a, the MC is equal to the MR, and the load carrying capability benefit reaches the global optimum. When the reliability constraint of electricity continues to be relaxed, the MR is zero. Because the ratio of electric load to heat load is fixed, if the load carrying capability continues to increase, the reliability of heat will not meet the constraint. Set the reliability constraint of heat to 30MWh/a, when the reliability constraint of electricity is relaxed to 32.1MWh/a, the MR falls to zero. This is because the reliability constraint of heat is too strict, so the load carrying capability benefit cannot reach the global optimum. For such cases, the optimization strategy for the system is to relax the reliability constraint of heat, to improve the benefit. Set the reliability constraint of heat to 60MWh/a, when the reliability constraint of electricity is relaxed easier than 53.9MWh/a, the load carrying capability is still increasing. But MC is greater than MR at this time, it is uneconomic. For such cases, the optimization strategy is to contract the reliability constraint of heat.

(2) Relationship between IDR ratio and load carrying capability benefit

By fixing the reliability constraint of electricity and heat to 53.9MWh/a and 30MWh/a respectively, the relationship between electric DR ratio and load carrying capability benefit is calculated when the heat DR ratio is set to 9.8%, 5%, and 15% respectively. The results are shown in Fig. 12.

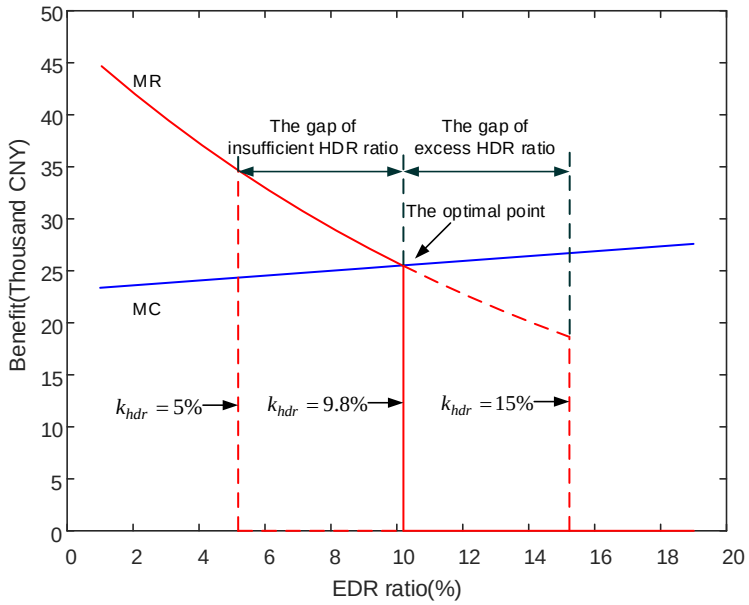

Fig. 12 The relationship between DR ratios and load carrying capability benefit

The increase of DR ratio will lead to the increase of load carrying capability, so that more load participate in DR. Therefore, when the DR ratio increases, the MC will also increase. When the heat DR ratio is 9.8%, the MR decreases with the increase of electric DR ratio. Until the electric DR ratio is 10.2%, the MC is equal to the MR, and the load carrying capability benefit reaches the global optimum. When the electric DR ratio continues to increase, the MR is zero. The principal is the same as that in the previous paragraph. Set the heat DR ratio to 5%, when the electric DR ratio increases to 5.1%, the MR falls to zero. For such cases, the optimization strategy is to increase the heat DR ratio. Set the heat DR ratio to 15%, when the electric DR ratio is more than 10.2%, the MC is greater than MR. For such cases, the optimization strategy

is to decrease the heat DR ratio.

(3) Calculation result of load carrying capability benefit considering uncertainties of load growth

According to the method proposed in Section 3.1, each point on the boundary of load carrying capability interval corresponds to a possible future scenario. The benefit of load carrying capability considering uncertainties can be obtained by calculating the benefit and probability of each point on the boundary of load carrying capability interval. Taking feeders 2 and 4 as an example, the existing industrial load is 4MW and the residential load is 3MW. The probability density distribution of the upper boundary of the load carrying capability interval can be calculated. The expectation vector is $\boldsymbol{\mu}=(y_2^0, y_4^0)=(4,3)$, it means the expectation is the industrial load and the residential load growth evenly according to the existing proportion. The standard deviation is 1/3 of the distance between the farthest point on the upper boundary and the expectation vector. The selection principle of standard deviation is the interval (-3σ, +3σ) contains 99.7% probability in a normal distribution. The probability density distribution of the boundary is shown in Fig. 13. Point O represents the existing load. The polygon OABCD is load carrying capability interval. The broken line BCD is the upper boundary of the interval. The blue curve is the probability density distribution on BCD. With the probability density distribution, the benefit of load carrying capability can be calculated based on Eqs. (30)-(32).

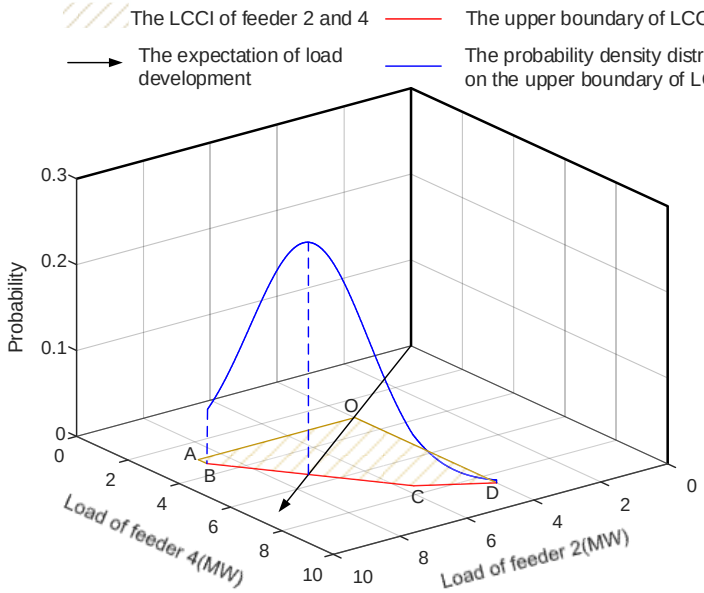

Fig. 13 The probability density distribution of the upper boundary

4.4 Result of linearization

According to Section 3.2, the LOEE of feeder 1 is related to the electric DR ratio and the load of feeder 1 and feeder 3. Its linear relationship is solved when electric DR ratio is fixed to 10%. Based on the piecewise linearization method proposed in this paper , when $y_1+y_3 \le C_3$, the LOEE of feeder 1 can be represented as:

$$R_{\mathrm{LOEE},1}=1.5127y_1 \tag{49}$$

The coefficient of determination R^2=0.9975, F value is 7645.7, p-value is $5.18*10^{-121}$.

When $y_1+y_3 > C_3$, the LOEE of feeder 1 can be represented as:

$$R_{\mathrm{LOEE},1}=7.7366-0.9481y_1-2.4168y_3+0.181y_1^2+0.3649y_1y_3+0.1844y_3^2 \tag{50}$$

The coefficient of determination R^2=0.9818, F value is 1014.3, p-value is $4.08*10^{-80}$.

The calculation results show that the linearization method proposed in this paper has good accuracy. The sampling points and the linear relationship fitting by the least square method is shown in Fig. 14. The blue points are the sample points calculated by the Monte Carlo simulation method. The mesh is calculated by the linearization method proposed in Section 3.2.

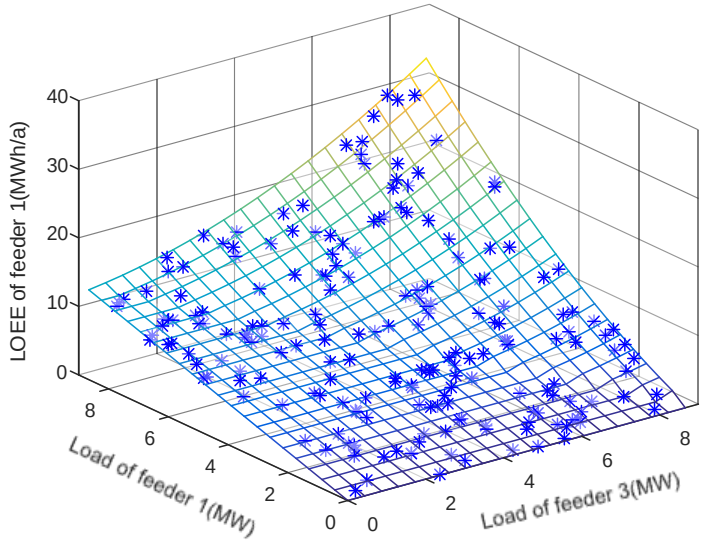

Fig. 14 Result of linearization

5 Conclusions

To evaluate the optimal value of load carrying capability for REHESs, this paper defines energy supply capability, available capacity, and load carrying capability. Interval models are built to display these indices. The characteristics of the intervals are analyzed. Considering the relationship of load carrying capability benefit, IDR costs, and load curtailment penalty, an evaluation method of optimal load carrying capability considering uncertainties of load growth is proposed. Because the lower-layer model is a very complex nonlinear problem, it is long time-comsuming. A linearization method for reliability calculation is proposed. The computation efficiency is greatly enhanced. The method proposed in this paper can calculate the reliability constraints and IDR ratios under the condition of optimal operation economy. The conclusions drawn in this paper are as follows:

(1) Relaxing reliability constraints or increasing IDR ratios can improve load carrying capability.

(2) If the load characteristics of various users are complementary, the load carrying capability will be greater than the available capacity.

(3) When the LOEE of one energy resource reaches the upper limit of the reliability constraint, load carrying capability will not increase with further relaxation of the reliability constraints of other energy resources or increase of IDR ratios. It is important to reasonably configure reliability constraints and IDR ratios.

The future work will consider the impact of renewable energy generation uncertainty on reliability and load carrying capability.

Acknowledgements

This work was supported by the National Natural Science Foundation of China (Grant NO. 51777133).

Reference

[1] Mohammad Shamsuzzaman, Ahm Shamsuzzoha, Ahmed Maged, Salah Haridy, Hamdi Bashir, Azharul Karim. Effective monitoring of carbon emissions from industrial sector using statistical process control[J]. Applied Energy, 2021, 300:117352.

[2] Houhe Chen,Ting Zhang,Rufeng Zhang,Tao Jiang,Xue Li,Guoqing Li. Interval optimal scheduling of integrated electricity and district heating systems considering dynamic characteristics of heating network[J]. IET Energy Systems Integration, 2020(2): 179-186.

[3] Kening Chen, Wenchuan Wu, Boming Zhang, Sasa Djokic, Gareth P. Harrison. A Method to Evaluate Total Supply Capability of Distribution Systems Considering Network Reconfiguration and Daily Load Curves[J]. IEEE Transactions on Power Systems, 2016(31), 3:2096-2104.

[4] Rafael S. Pinto, Clodomiro Unsihuay-Vila, Fabricio H. Tabarro. Coordinated operation and expansion planning for multiple microgrids and active distribution networks under uncertainties[J]. Applied Energy, 2021, 297(11):117108.

[5] Weiwei Xu, Dan Zhou, Xiaoming Huang, Boliang Lou, Dong Liu. Optimal allocation of power supply systems in industrial parks considering multi-energy complementarity and demand response[J]. Applied Energy, 2020, 275:115407.

[6] Yixin Yu, Yanli Liu, Chao Qin, Tiankai Yang. Theory and method of power system integrated security region irrelevant to operation states: an introduction[J]. Engineering, 2020, 6:754-777.

[7] Jhonatan S. Ferreira, Edimar J. de Oliveira, Arthur N. de Paula, Leonardo W. de Oliveira, João A. Passos Filho. Optimal power flow with security operation region[J]. International Journal of Electrical Power & Energy Systems. 2021, 124:106272.

[8] Wei Dai, Zhifang Yang, Juan Yu, Ke Zhao, Shiyang Wen, Wei Lin, et al. Security region of renewable energy integration: Characterization and flexibility[J]. Energy, 2019, 187:115975.

[9] Chenhui Song, Jun Xiao, Guoqiang Zu, Ziyuan Hao, Xinsong Zhang. Security region of natural gas pipeline network system: Concept, method and application[J]. Energy, 2021, 217:119283.

[10] Tao Jiang, Rufeng Zhang, Xue Li, Houhe Chen, Guoqing Li. Integrated energy system security region: Concepts, methods, and implementations[J]. Applied Energy, 2021, 283:116214.

[11] Jia Su, Hsiao-Dong Chiang, Ning Zhou. Toward complete characterization of the steady-state security region for the electricity-gas integrated energy system [J]. IEEE Transactions on Smart Grid, 2021, 12(4):3004-3015.

[12] Jia Su, Hsiao-Dong Chiang, Luís Fernando Costa Alberto. Two-time-scale approach to characterize the steady-state security region for the electricity-gas integrated energy system[J]. IEEE Transactions on Power Systems, 2021,36(6): 5863-5873.

[13] Linquan Bai, Fangxing Li, Tao Jiang, Hongjie Jia. Robust scheduling for wind integrated energy systems considering gas pipeline and power transmission N-1 contingencies[J]. IEEE Transactions on Power Systems, 2017, 32(3):1582-1584.

[14] Liu Liu, Dan Wang, Kai Hou, Hongjie Jia, Siyuan Li. Region model and application of

regional integrated energy system security analysis[J]. Applied Energy, 260:114268.
[15] Wujing Huang, Ning Zhang, Chongqing Kang , Mingxuan Li, Molin Huo. From demand response to integrated demand response: review and prospect of research and application[J]. Protection and Control of Modern Power Systems, 2019, 4:12.
[16] Peng Li, Zixuan Wang, Jiahao Wang, Weihong Yang, Tianyu Guo, Yunxing Yin. Two-stage Optimal Operation of Integrated Energy System Considering Multiple Uncertainties and Integrated Demand Response[J]. Energy, 2021, 225(4):120256.
[17] Ahmarinejad A . A Multi-objective Optimization Framework for Dynamic Planning of Energy Hub Considering Integrated Demand Response Program[J]. Sustainable Cities and Society, 2021(1):103136.
[18] Liangce He, Zhigang Lu, et al. Environmental economic dispatch of integrated regional energy system considering integrated demand response[J]. International Journal of Electrical Power & Energy Systems, 2020,116:105525.
[19] Xiaohui Yang, Zaixing Chen, Xin Huang, Ruixin Li, Shaoping Xu, Chunsheng Yang. Robust capacity optimization methods for integrated energy systems considering demand response and thermal comfort[J]. Energy, 2021, 221:119727.
[20] Hossein Aghamohammadloo, Valiollah Talaeizadeh, Kamran Shahanaghi, Jamshid Aghaei, Heidarali Shayanfar, Miadreza Shafie-khah, et al. Integrated Demand Response programs and energy hubs retail energy market modelling[J]. Energy, 2021, 234:121239.
[21] Rujing Yan, Jiangjiang Wang, Shuaikang Lu, Zherui Ma, Yuan Zhou, Lidong Zhang, et al. Multi-objective two-stage adaptive robust planning method for an integrated energy system considering load uncertainty[J]. Energy and Buildings, 2021, 235(2):110741.
[22] Xinwei Shen, Qinglai Guo, Hongbin Sun. Regional Integrated Energy System Planning considering Energy Price Uncertainties: A Two-stage Stochastic Programming Approach[J]. Energy Procedia, 2019, 158:6564-6569.
[23] Matija Kostelac, Ivan Pavić, Ning Zhang, Tomislav Capuder. Uncertainty modelling of an industry facility as a multi-energy demand response provider[J]. Applied Energy, 2022,307:118215.
[24] Wenxia Liu, Yuchen Huang, Zhengzhou Li, Yue Yang, Fang Yi. Optimal allocation for coupling device in an integrated energy system considering complex uncertainties of demand response[J]. Energy, 2020, 198(5):117279.
[25] Yu Fu, Haiyang Lin, Cuiping Ma, Bo Sun, Hailong Li, Qie Sun, et al. Effects of uncertainties on the capacity and operation of an integrated energy system[J]. Sustainable Energy Technologies and Assessments, 2021:101625.
[26] Shaoyun Ge, Yuchen Cao, Hong LIU, Xingtang He, Zhengyang Xu, Jifeng Li. Energy supply capability of regional electricity-heating energy systems: definition, evaluation method, and application[J]. International Journal of Electrical Power & Energy Systems, 2021, 107755.
[27] Albert Vexler. Univariate likelihood projections and characterizations of the multivariate normal distribution[J]. Journal of Multivariate Analysis, 2020,179:104643.
[28] Mehdi Amiri, Narayanaswamy Balakrishnan. Hessian and increasing-Hessian orderings of scale-shape mixtures of multivariate skew-normal distributions and applications[J]. Journal of Computational and Applied Mathematics, 2022, 402:113801.
[29] Hong Liu, Yue Zhao, Shaoyun Ge, Peng Zhang, Wei Liu, Xiaoguang Qi, et al. Reliability evaluation of regional energy Internet considering electricity–gas coupling and coordination between energy stations. IET Energy Systems Integration, 2021(3): 238-249.
[30] Lin Chen, Jianxiao Wang, Zhaoyuan Wu, Gengyin Li, Ming Zhou, Peng Li, et al. Communication reliability-restricted energy sharing strategy in active distribution networks[J]. Applied Energy, 2021, 282:116238.

[31] Ron N. Allan, Roy Billinton, I. Sjarief, Lalit Goel, K. S. So. A reliability test system for educational purposes-basic distribution system data and results[J]. IEEE Transactions on Power Systems, 1991, 6(2):813-820.
[32] Xuezhi Liu, Jianzhong Wu, Nick Jenkins, Audrius Bagdanavicius. Combined analysis of electricity and heat networks[J]. Applied Energy, 2016, 162:1238-1250.

Appendix